AGU PUBLICATIONS

JGR

Journal of Geophysical Research: Atmospheres

RESEARCH ARTICLE
10.1002/2014JD022380

Key Points:
- We estimated the monthly evapotranspiration at four large basins in Tibetan Plateau
- We evaluated five global evapotranspiration products with a water balance method
- Seasonal evapotranspiration trends (1983–2006) were detected from corrected data

Correspondence to:
X. Li,
lixiuping@itpcas.ac.cn

Citation:
Li, X., L. Wang, D. Chen, K. Yang, and A. Wang (2014), Seasonal evapotranspiration changes (1983–2006) of four large basins on the Tibetan Plateau, *J. Geophys. Res. Atmos.*, *119*, 13,079–13,095, doi:10.1002/2014JD022380.

Received 12 AUG 2014
Accepted 31 OCT 2014
Accepted article online 10 NOV 2014
Published online 4 DEC 2014

Seasonal evapotranspiration changes (1983–2006) of four large basins on the Tibetan Plateau

Xiuping Li[1], Lei Wang[1,2], Deliang Chen[3], Kun Yang[1,2], and Aihui Wang[4]

[1]Key Laboratory of Tibetan Environment Changes and Land Surface Processes, Institute of Tibetan Plateau Research, Chinese Academy of Sciences, Beijing, China, [2]CAS Center for Excellence in Tibetan Plateau Earth Sciences, Beijing, China, [3]Department of Earth Sciences, University of Gothenburg, Gothenburg, Sweden, [4]Nansen-Zhu International Research Center, Institute of Atmospheric Physics, Chinese Academy of Sciences, Beijing, China

Abstract Lack of reliable historical basin-scale evapotranspiration (*ET*) estimates is a bottleneck for water balance analyses and model evaluation on the Tibetan Plateau (TP). This study looks at four large basins on the TP to develop a general approach suitable for large river basins to estimate historical monthly *ET*. Five existing global *ET* products are evaluated against monthly *ET* estimated by the water balance method as a residual from precipitation (*P*), terrestrial water storage change (ΔS), and discharge (*R*). The five *ET* products exhibit similar seasonal variability, despite of the different amounts among them. A bias correction method, based on the probability distribution mapping between the reference *ET* and the five products during 2003–2012, effectively removes nearly all biases and significantly increases the reliability of the products. Then, the surface water balance changes for the four basins are analyzed based on the corrected *ET* products as well as observed *P* and *R* during 1983–2006. A trend analysis shows an upward trend for *ET* in the four basins for all seasons during the past three decades, along with the regional warming, as well as a dominating increasing trend in *P* and negative trend in *R*.

1. Introduction

Evapotranspiration (*ET*) is a critical process that determines terrestrial water budget and exchanges of surface energy. Global and regional climate changes [*Intergovernmental Panel on Climate Change Fifth Assessment Report (IPCC AR5)*, 2013; *Liu and Chen*, 2000; *Su et al*., 2013] have changed hydrological cycles and surface energy budgets [e.g., *Ohmura and Wild*, 2002; *Huntington*, 2006; *Gao et al*., 2007; *Yang et al*., 2011]. More importantly, *ET* is taken as an indicator for climate change, in particular for the accelerated hydrological cycle [*Brutsaert and Parlange*, 1998; *Ohmura and Wild*, 2002]. Accurately, quantifying the terrestrial water budget can help to improve our understanding of global and regional water cycle changes and the role of *ET* in the hydrologic cycle. However, obtaining water budget components from ground-based measurements alone remains a challenge. As a result of high variability in time and space, *ET* is perhaps the most difficult and complicated component in the hydrological cycle and is especially difficult to measure [*Xu and Singh*, 2005].

The Tibetan Plateau (TP), also called the "Asian Water Tower," is essential to Asian monsoon evolvement and concurrent water-energy cycles. Shrinking glaciers at the headwaters of many prominent Asian rivers and changes in precipitation patterns caused by weakening Indian monsoons and strengthening westerlies [*Yao et al*., 2012] have all influenced the hydrologic cycle in this area [*Immerzeel et al*., 2010]. *Yang et al*. [2011] indicated that the surface water balance has changed in recent decades and that *ET* shows an overall increasing trend in the TP. However, their results were derived from a land surface model driven by meteorological observations only and lacked sufficient observations in the TP.

There are a number of methods to estimate *ET*, including micrometeorological measurements [e.g., *Rana and Katerji*, 2000], climatology water balance [e.g., *Gao et al*., 2007], remote sensing-based methods [e.g., *Vinukollu et al*., 2011a, 2011b; *Zhang et al*., 2010; *Ferguson et al*., 2010; *Mu et al*., 2007], and land surface models [e.g., *Yang et al*., 2011; *Zhou and Huang*, 2012]. However, these methods are often constrained by sparse measurement stations and a number of uncertainties involving input data and techniques, as well as by the model used [e.g., *Wang and Dickinson*, 2012]. The traditional water balance method provides another useful tool for estimating *ET* at the regional or basin scale [e.g., *Rodell et al*., 2004b; *Sheffield et al*., 2009; *Gao et al*., 2010]. The newly launched Gravity Recovery and Climate Experiment (GRACE) satellite [*Wahr et al*., 2004;

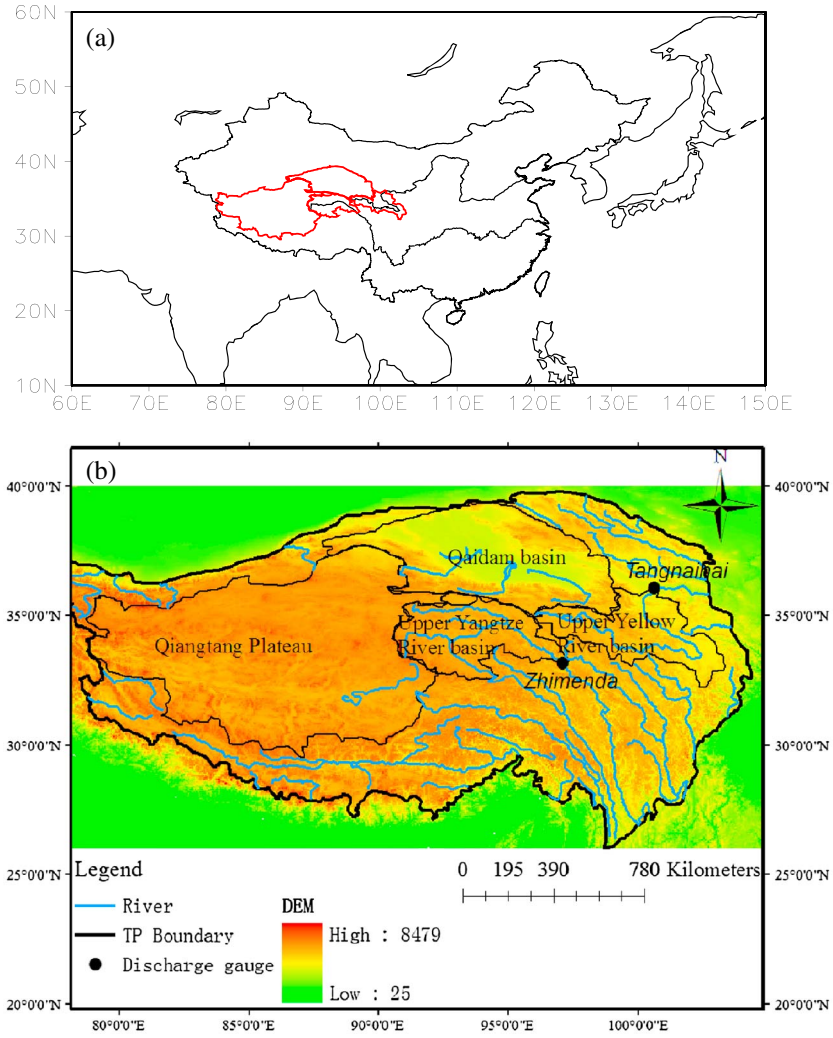

Figure 1. (a) Location of the study region in China. (b) Distributions of two discharge gauge stations with closed circles. The shades illustrate the elevation from Shuttle Radar Topography Mission digital elevation model (DEM) (m).

Tapley et al., 2004] is a perfect fit for water budget studies because it is a horizontally and vertically integrated quantity [*Rodell and Famiglietti*, 1999]. In the past decades, a number of studies have focused on global and regional quantifications of *ET* by the water balance method [e.g., *Ramillien et al*., 2006; *Swenson and Wahr*, 2006a; *Sheffield et al*., 2009; *Rodell et al*., 2004b]. Although the uncertainties in the GRACE data are generally much greater owing to its coarse spatial resolution, it still is an effective way to study the water balance at the basin scale. Recently developed filtering technique designed to selectively remove correlated errors in the GRACE spectral coefficients significantly improves the spatial resolution of the GRACE water storage estimates [*Swenson et al*., 2006]. Lately, scaled gridded data, accompanied with provided leakage and GRACE measurement errors and gain factors, may be finer spatial scales to achieve accurate results [*Landerer and Swenson*, 2012].

Over the past decade, a large number of studies focused on potential evapotranspiration (or pan evaporation) in China [*Chen et al*., 2005; *Xu et al*., 2006] and on the TP [e.g., *Zhang et al*., 2007; *Liu et al*., 2011]. Several regional studies in the world have demonstrated that potential evapotranspiration or pan evaporation can have a different change compared to the actual evapotranspiration under climate change [*Brutsaert and Parlange*, 1998; *Hobbins et al*., 2004; *Lawrimore and Peterson*, 2000; *Golubev et al*., 2001]. *Gao et al*. [2007] studied the variations of potential evapotranspiration and actual

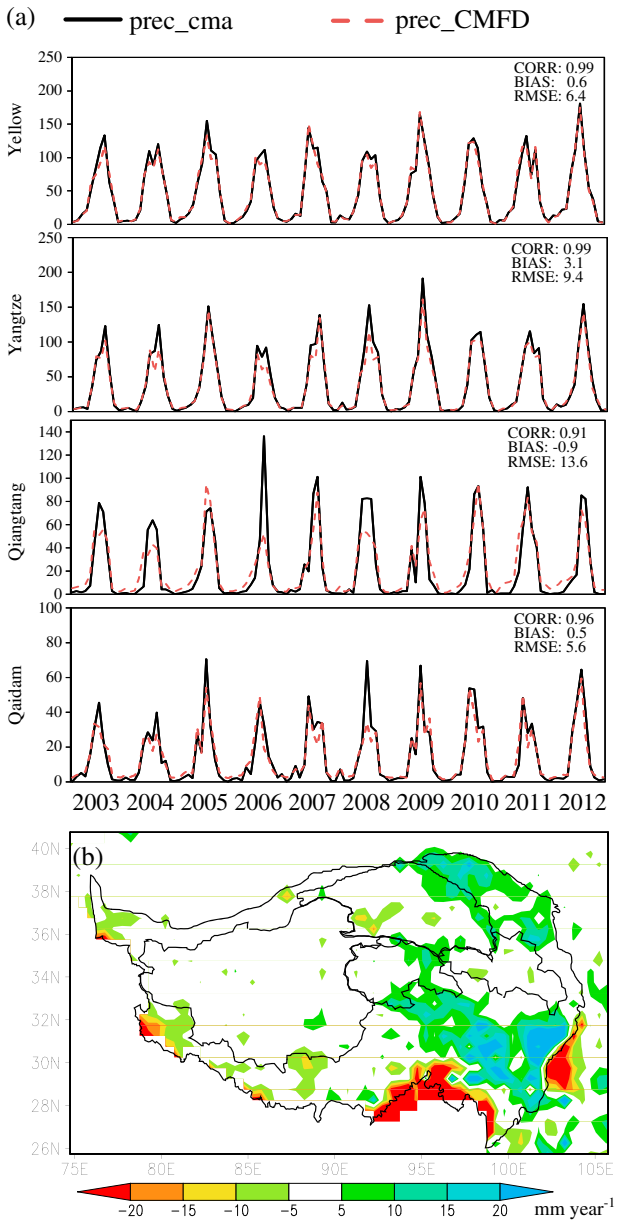

Figure 2. (a) Comparison of the monthly precipitation (mm month^{-1}) from CMA (prec_CMA) and from China Meteorological Forcing Data Set (prec_CMFD), for domain-averaged time series on the four basins and (b) for annual mean difference (prec_CMA minus prec_CMFD) on the whole TP.

evapotranspiration over China during 1960–2002 and obtained similar conclusion. However, the number of stations over the TP in their study was too few to draw a general conclusion for the TP. Besides, the approach may be too simple to get an accurate estimate.

Under the background of global climate change over the last decades, what was the actual change in the evapotranspiration on the TP? To address the question effectively, a hydrological water balance method can be used to reveal the variation of actual *ET* on the TP. Recently, *Xue et al.* [2013] had used the method to estimate annual *ET* and then evaluated existing *ET* products on the TP at the annual scale.

To further understand the seasonal variations of water cycles and their response to climate changes on the TP, monthly or seasonal *ET* products are needed. In this study, we use the basin-scale water balance method in hydrology to estimate monthly *ET* as the reference *ET* for large basins on the TP. Then, we propose a simple method to correct monthly *ET* fields from several global *ET* products with the help of the reference *ET*. Finally, long-term (1983–2006) variations of the basin-scale water balance in four seasons are investigated by means of the corrected *ET* estimates, along with the observed *P* and *R*.

The paper is structured as follows. In section 2, we describe the study region, followed by the data and methodology. Section 3 presents the results of the estimation of *ET* by the water balance

Table 1. Overview of the Five Global *ET* Products

Data Sets	Category	Spatial Resolution	Temporal Extent	References
Zhang_ET	Penman–Monteith method	8 km	1983–2006	*Zhang et al.* [2010]
MODIS_ET	Penman–Monteith method	1 km	2000–2012	*Mu et al.* [2007]
GLDAS1_ET	land surface model	1°×1°	1948–2012	*Rodell et al.* [2004a]
GLDAS2_ET	land surface model	1°×1°	1948–2010	*Rodell et al.* [2004a]
JRA_ET	reanalysis	T106 Gaussian	1979–2012	*Onogi et al.* [2007]

Table 2. Correlation Coefficients (CORR) Among Monthly Domain-Averaged TWSA (Total Water Storage Anomaly) and ΔSs (Total Water Storage Changes) From CSR, GFZ, and JPL Centers, as Well as the Standard Deviations (SD) (mm month^{-1}) of Monthly Domain-Averaged TWSA and ΔS for the Four Basins on the TP

		TWSA				ΔS			
		Yellow	Yangtze	Qiangtang	Qaidam	Yellow	Yangtze	Qiangtang	Qaidam
CORR	CSR and GFZ	0.91	0.91	0.86	0.89	0.82	0.79	0.75	0.73
	CSR and JPL	0.89	0.85	0.71	0.79	0.86	0.79	0.65	0.69
	GFZ and JPL	0.85	0.79	0.58	0.72	0.77	0.69	0.54	0.51
SD	CSR	42.8	23.2	23.0	9.5	21.9	11.3	11.0	3. 9
	GFZ	46.9	25.4	26.0	10.6	24.7	13.5	14.1	5.1
	JPL	40.3	22.8	24.2	9.6	20.2	10.5	12.1	4.1

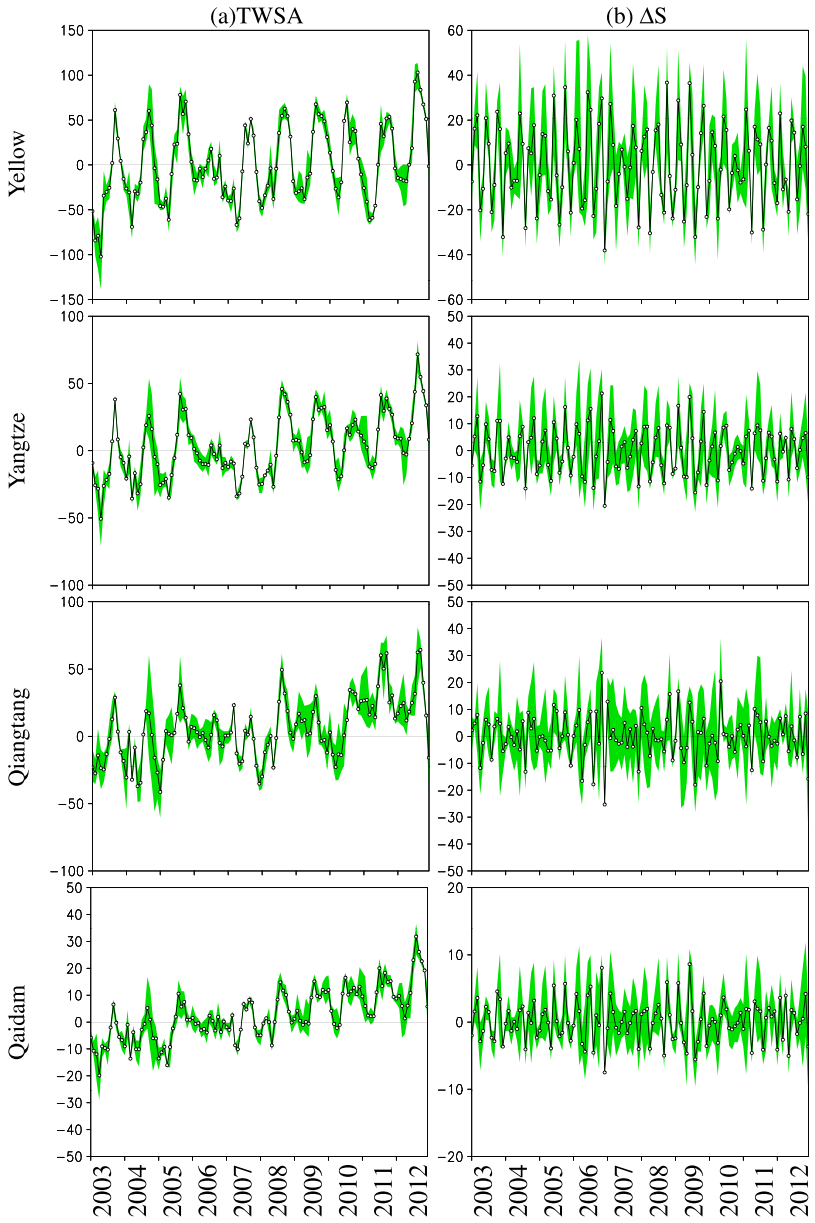

Figure 3. Monthly domain-averaged (a) TWSA (total water storage anomaly) (mm month^{-1}) and (b) ΔS (mm month^{-1}) over the four basins. The shades indicate the range determined by data sets from CSR, GFZ, and JPL centers, while the lines represent the mean of the three.

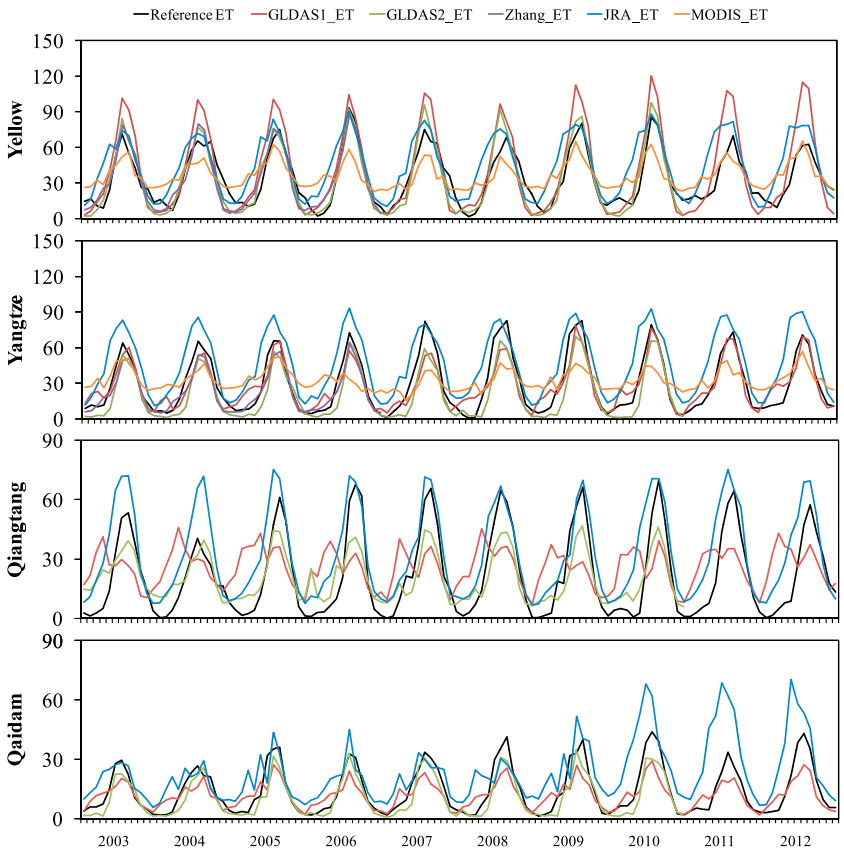

Figure 4. Comparison of the domain-averaged values between the five global *ET* products (mm month^{-1}) and the reference *ET* (mm month^{-1}) estimated by the water balance method for the four basins from January 2003 to December 2012. The statistical values for comparison are shown in Table 3.

method and analysis of the long-term water balance for the four basins. Section 4 contains the conclusions and discussions.

2. Study Regions, Data Sets, and Method

2.1. Study Regions

Two types of basins on the TP, with and without surface runoff flowing out of the basin, are involved in this work. The first type includes the upper Yellow and Yangtze River basins (see Figure 1), determined by the stream systems extracted from the digital elevation model(DEM), with outlets at Zhimenda for the upper Yangtze River and Tangnaihai for the upper Yellow River. The upper Yellow River and Yangtze River

Table 3. Bias (mm), RMSE (mm), and Correlation Coefficient of the Five Monthly *ET* Products in Comparison With the Reference *ET* (mm) Estimated From the Water Balance for the Four Basins on the TP[a]

	Yellow				Yangtze				Qiangtang				Qaidam			
Data Sets	Mean	BIAS	RMSE	CORR	Mean	BIAS	RMSE	CORR	Mean	BIAS	RMSE	CORR	Mean	BIAS	RMSE	CORR
Reference *ET*	34.0				29.4				22.3				14.3			
GLDAS1_ET	40.0	6.0	14.7	0.96	28.0	**−1.4**	9.5	0.92	25.8	3.6	21.4	0.28	12.0	**−2.2**	7.3	0.88
GLDAS2_ET	32.9	−1.2	7.1	**0.97**	20.3	−8.9	11.8	0.95	20.5	**−1.5**	**11.8**	**0.92**	10.7	−3.5	**5.6**	**0.93**
JRA_ET	44.5	10.5	16.4	0.87	46.7	17.2	20.4	0.91	33.1	10.8	14.4	0.91	23.3	9.0	14.1	0.70
Zhang_ET	32.8	**−0.8**	**5.5**	0.95	23.2	−3.7	**7.1**	**0.96**								
MODIS_ET	36.5	2.5	17.1	0.86	32.4	3.0	18.2	0.76								

[a]Smaller BIAS and RMSE and larger correlation coefficients are in boldface.

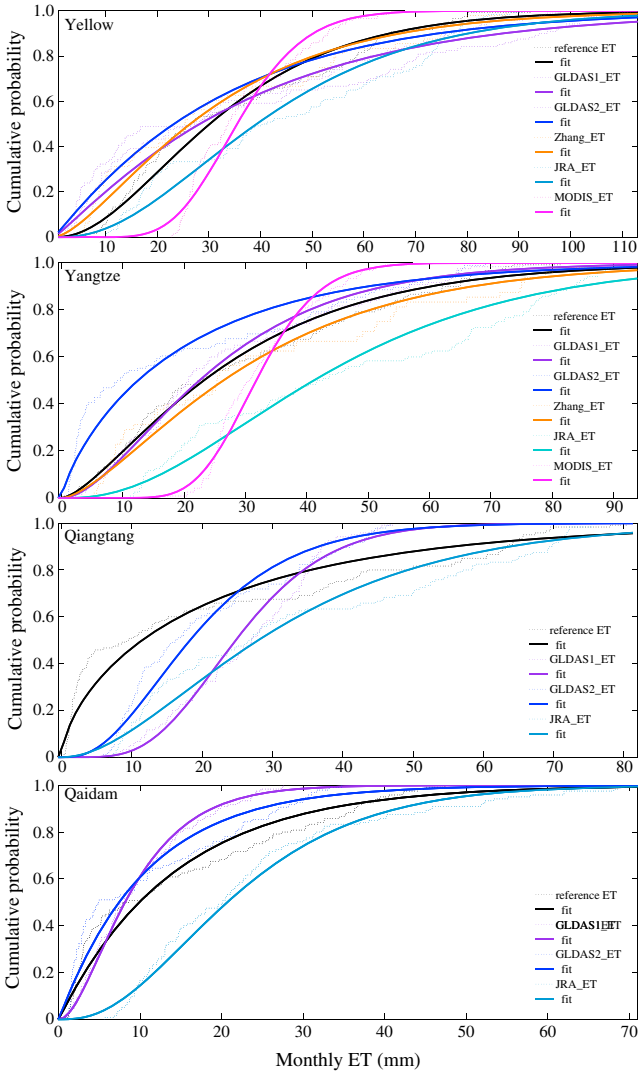

Figure 5. Distribution of the monthly domain-averaged *ET* values from the reference *ET* (mm month^{-1}) and *ET* products (mm month^{-1}) for the period of 2003–2012. The dashed lines and the solid lines represent the values and their gamma distribution fitting, respectively.

basins have total areas of 121,972 and 137,704 km^2, respectively. The main soil types are alpine cold desert, alpine meadow, alpine steppe, mountain meadow, gray cinnamonic, chestnut, swamp, and aeolian [*Bing et al.*, 2012]. The second type includes the Qiangtang Plateau and the Qaidam Basin, with total areas of 700,000 and 257,768 km^2, respectively. They are the highest inland basins with many rivers and lakes in China. Water in the two inland basins evaporates after flowing into the lakes. The climate of the four basins is classified as semiarid and subhumid plateau continental, with distinct wet and dry seasons. The study region is strongly influenced by the summer Indian monsoon and East Asian monsoon during summer [*Yao et al.*, 2012]. The geographical distribution of the basins and hydrological stations are shown in Figure 1.

2.2. Data Sets

2.2.1. Precipitation and Runoff Data

Precipitation (*P*) from the National Meteorological Information Center of the China Meteorological Administration (CMA) and observed discharge (*R*) for Tangnaihai and Zhimenda are used to estimate the *ET* by the water balance method. The precipitation data are spatially interpolated by the Thin Plate Spline method from 2400 ground stations to generate gridded monthly data sets with a horizontal resolution

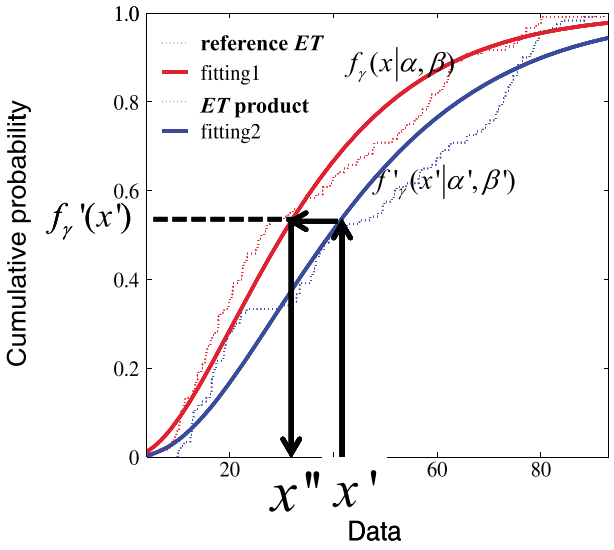

Figure 6. Schematic diagram of the first step in the bias correction method. The red lines represent the values and their fittings from the reference *ET* estimated by the water balance method, while the blue lines from the *ET* product. The corresponding functions for the reference *ET* and the *ET* product are also expressed in the figure. Parameters *x*′ and *x*″ are the *ET* values before and after the bias correction at the first step.

of 0.5°×0.5° across China (18–54°N, 72–136°E). The data are available from January 1961 to present and can be downloaded from the China Meteorological Data Sharing Service System (http://cdc.cma.gov.cn/home.do).

Due to sparse distribution of precipitation stations on the TP, the representativeness of this precipitation data is explored through comparing with another precipitation data from China Meteorological Forcing Data Set (CMFD) [*He and Yang*, 2011]. This precipitation from CMFD with higher temporal resolution (3-hourly) and spatial resolution (0.1°) was produced through merging CMA station data, Tropical Rainfall Measuring Mission satellite precipitation data (3B42), and the Global Land Data Assimilation System (GLDAS) precipitation data. It was found that domain-averaged *P* values from CMA were comparable to those from CMFD forcing data (shown in Figure 2a). The mean annual differences between CMA and CMFD data for the four basins range from −5.0 mm to 5.0 mm (shown in Figure 2b), which is considered small. Therefore, the *P* values from CMA, generated completely by station data, are considered of reasonable quality for the following analysis.

2.2.2. Global *ET* Products

Five *ET* products were evaluated (details of the five *ET* products are presented in Table 1). Zhang_ET from *Zhang et al.* [2010] and MODIS_ET from Moderate Resolution Imaging Spectroradiometer (MODIS) [*Mu et al.*, 2007] are produced by the Penman–Monteith method. Note that these two products do not cover the whole TP. *ET* from the Global Land Data Assimilation System with Noah Land Surface Version 1 (hereafter GLDAS1_ET) [*Rodell et al.*, 2004a] and Noah Land Surface Version 2 (hereafter GLDAS2_ET) [*Rodell et al.*, 2004a] are also evaluated. GLDAS1_ET is produced by constantly updated meteorological data, while GLDAS2_ET is forced by the Princeton meteorological forcing data set [*Sheffield et al.*, 2006] for the period of 1948–2010, which is more suitable for analyzing the long-term trends. The last *ET* product is from the Japanese 25 year Reanalysis (JRA) (hereafter JRA_ET) [*Onogi et al.*, 2007]. JRA is a high-quality, homogeneous data set in space and time for land surface hydrological cycles, proved by previous study [e.g., *Takahashi et al.*, 2006; *Nakaegwa*, 2008; *Tosiyuki*, 2008].

2.2.3. GRACE Data

The terrestrial water storage changes (ΔSs) are derived from the Gravity Recovery and Climate Experiment (GRACE) land data [*Tapley et al.*, 2004]. The descriptions of present status and solving of GRACE gravity field solutions are presented in previous study [*Tapley et al.*, 2004; *Rodell and Famiglietti*, 1999; *Swenson and Wahr*, 2002, 2006a, 2006b; *Wahr et al.*, 2004]. Although the spatial resolution of GRACE data is around a few hundred kilometers, a reasonable agreement between GRACE estimated and in situobservation has been found [*Yeh et al.*, 2006], and the usefulness of the data in hydrological applications has already been demonstrated for basin scale [*Rodell and Famiglietti*, 2002; *Longuevergne et al.*, 2010; *Landerer and Swenson*, 2012; *Xue et al.*, 2013; *Long et al.*, 2014].

Here RL05 gridded data (available on the GRACE Tellus website) are extracted to examine the domain-averaged changes of terrestrial water storage for the basins on the TP, which are processed at the Center for Space Research (CSR), University of Texas; the Jet Propulsion Laboratory (JPL); and the GeoForschungsZentrum (GFZ). A destriping filter and a glacial isostatic adjustment correction have been

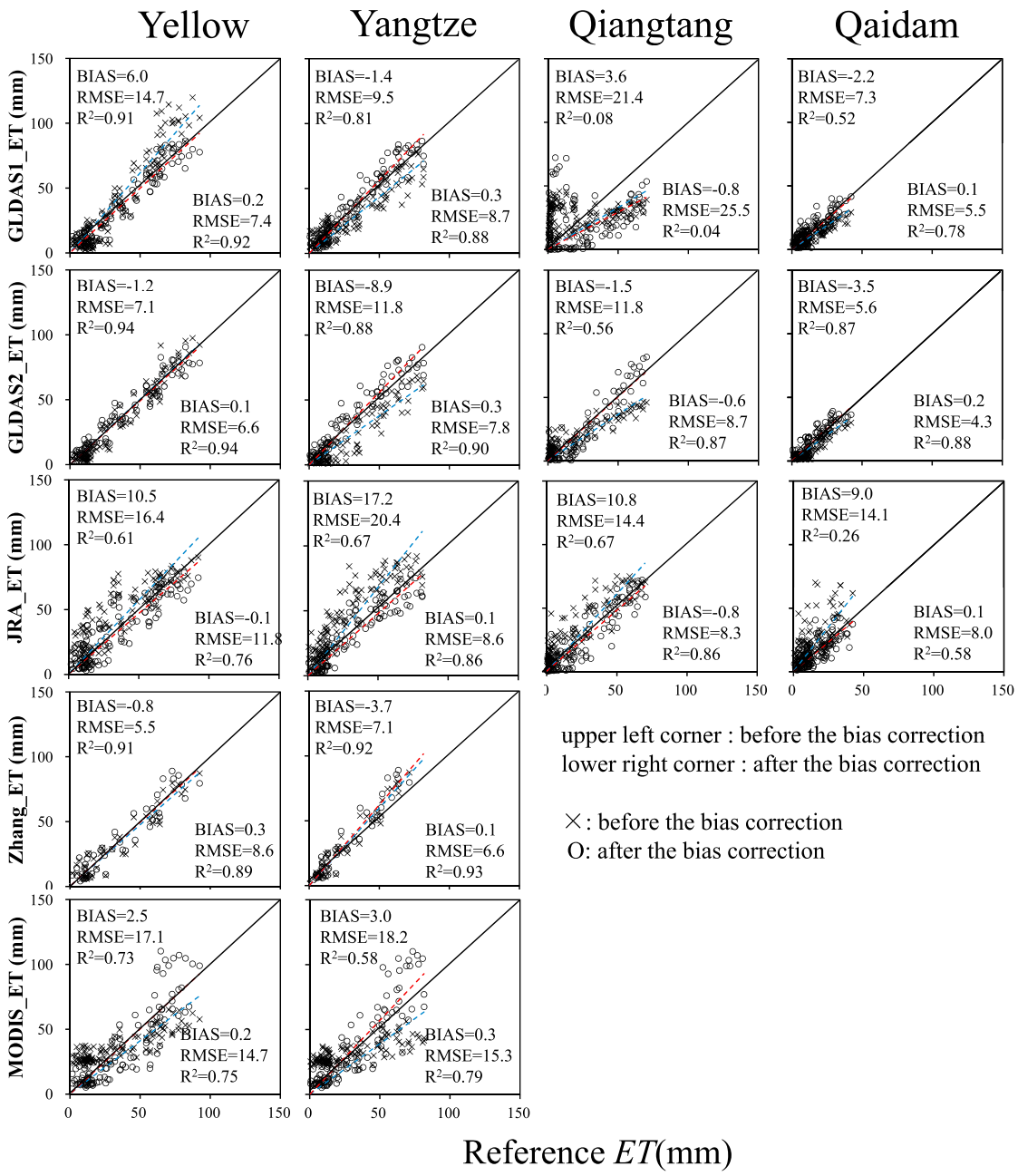

Figure 7. Comparison of the monthly *ET* products with the reference *ET* before and after the bias correction for the four basins on the TP.

applied to the data to minimize the error [*Landerer and Swenson*, 2012; *Swenson and Wahr*, 2006b]. However, each center follows different data processing methods, which might cause some differences in the solutions [*Klees et al*., 2007].

In order to explore the uncertainties of ΔS from RL05 products in estimating *ET* at the basin scale on the Tibetan Plateau, the terrestrial water storage anomaly (TWSA) and ΔS from the three processing centers (CSR, GFZ, and JPL) for the study regions are compared. Statistical values for the comparison are listed in Table 2. It was found that TWSA from the three centers showed an overall agreement, demonstrated by high temporal correlation coefficients and similar standard deviation of the monthly variation, providing some confidence to derive monthly ΔS for the water balance calculation. Figure 3 also shows the ranges of TWSA and ΔS, determined by GRACE data from the three centers and their means for

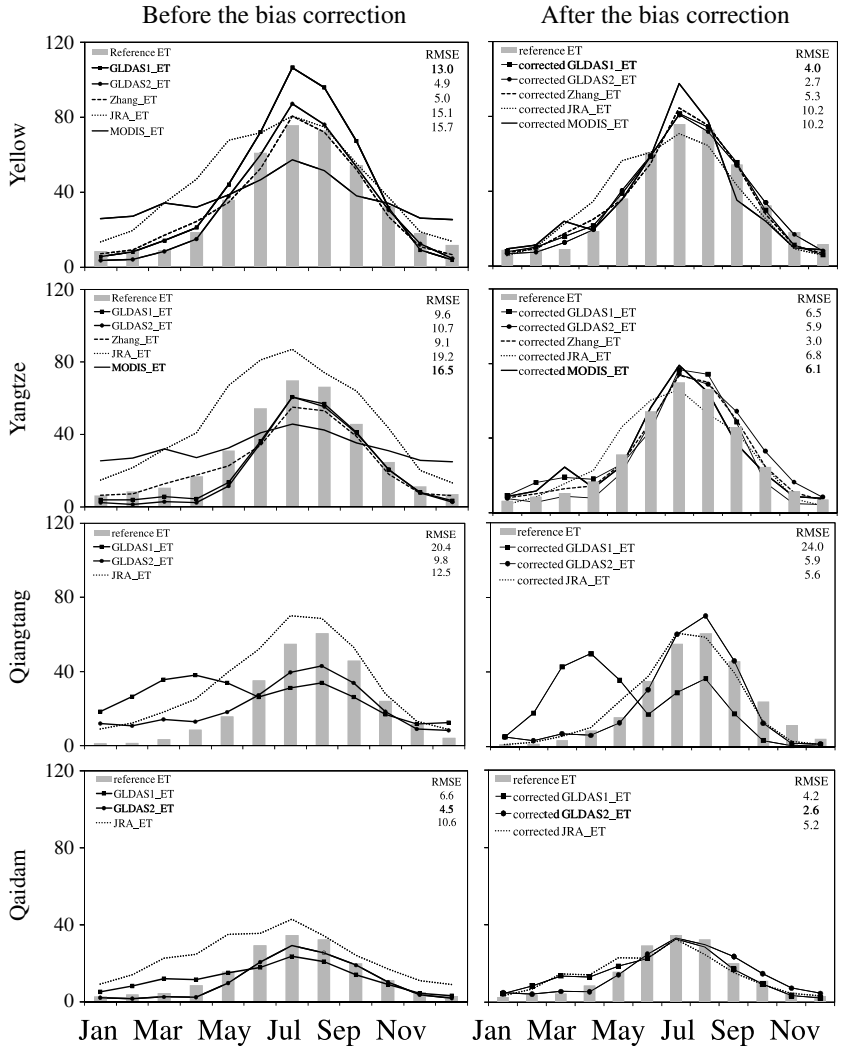

Figure 8. Seasonal cycle of the reference *ET* (mm month^{-1}) and the *ET* products (mm month^{-1}) before and after the bias correction in the four basins averaged for the period of 2003–2012. The RMSE values (mm month^{-1}) are shown in the upper right corner of the figures.

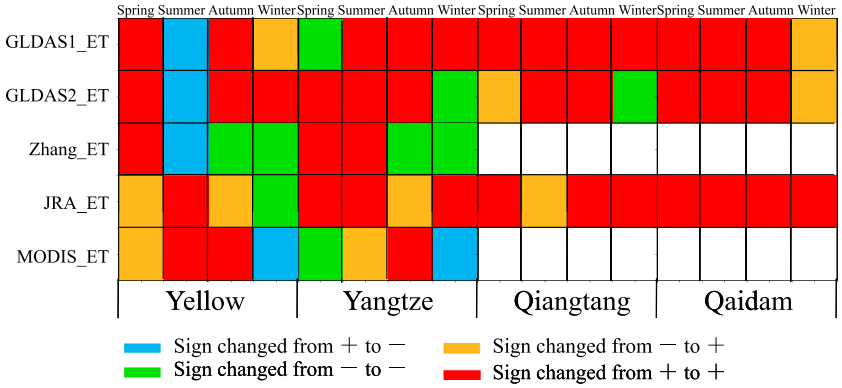

Figure 9. Changes in the sign of the correlation coefficient between the mean monthly reference *ET* from 2003 to 2012 and those from the five *ET* products before and after the bias correction for the four basins. The plus and minus signs indicate the positive and negative correlation coefficients, respectively.

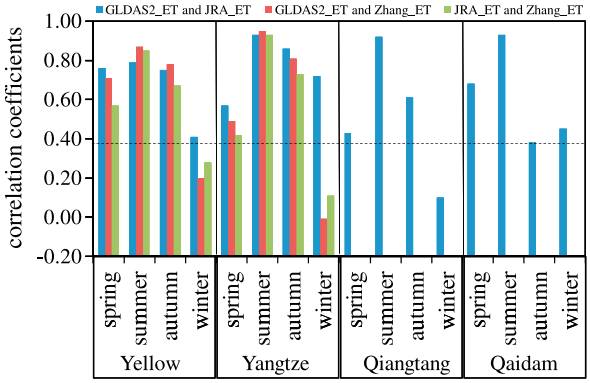

Figure 10. Correlation coefficients among seasonal mean-corrected *ET* products in the four basins during the period of 1983–2006. The dashed line represents the 95% significant level.

the four basins from January 2003 to December 2012. There are larger variations for TWSA and ΔS, especially for the upper Yellow River basin. Similar to the study by *Tang et al.* [2013], the GRACE products from the three processing centers are averaged to extract ΔS from January 2003 to December 2012 in our study to minimize the impact from individual errors of the three TWSA estimates.

2.3. Method

The traditional water balance method, shown in equation (1), is used to estimate *ET* (hereafter, reference *ET*) for the four basins [e.g., *Hobbins et al*., 2004; *Rodell et al*., 2004b; *Xue et al*., 2013].

$$ET = P - R - \Delta S \tag{1}$$

where P is the total precipitation (mm), R is the river discharge (mm), and ΔS is the change in terrestrial water storage (mm; including surface, subsurface, and groundwater changes).

Normally, P and R are obtained from in situ observation, and ΔS is assumed negligible over a long period (usually annual or longer time scale) [e.g., *Hobbins et al*., 2004; *Xue et al*., 2013]. But at the monthly scale, ΔS is not negligible and should be considered. For the inland basins (Qiangtang Plateau and Qaidam Basin), the discharge is zero, and the traditional water balance equation can be simplified to equation (2).

$$ET = P - \Delta S \tag{2}$$

Bias (BIAS), root-mean-square error (RMSE), and correlation coefficient (CORR) are used as evaluation criteria for the *ET* products against the reference *ET*, and they are defined as

$$\mathrm{BIAS} = \sum_{i=1}^{N}(A_i - B_i)/N \tag{3}$$

$$\mathrm{RMSE} = \sqrt{\sum_{i=1}^{N}(A_i - B_i)^2/N} \tag{4}$$

$$\mathrm{CORR} = \frac{\sum_{i=1}^{N}\left(A_i - \overline{A}\right)\left(B_i - \overline{B}\right)}{\sqrt{\sum_{i=1}^{N}\left(A_i - \overline{A}\right)^2}\sqrt{\sum\left(B_i - \overline{B}\right)^2}} \tag{5}$$

where N represents the number of months of the study period and A_i and B_i are from the monthly *ET* products and the reference *ET*, respectively.

As a result of the different horizontal resolutions among P, ΔS, and the five *ET* products, all data are consistently resampled to a 0.5°×0.5° grid for comparison in this study. To detect temporal trends for all time series data, a linear regression (least squares method) is used for the annual and seasonal basin-averaged values. The seasons considered are spring (March–May), summer (June–August), autumn (September–November), and winter (December–February).

3. Results

3.1. Evaluation of *ET* Products

In our study, we use the gridded P values provided by CMA, in situ observed R, and the estimated ΔS from GRACE to estimate *ET* by the water balance method. Figure 4 shows the monthly variations of the reference

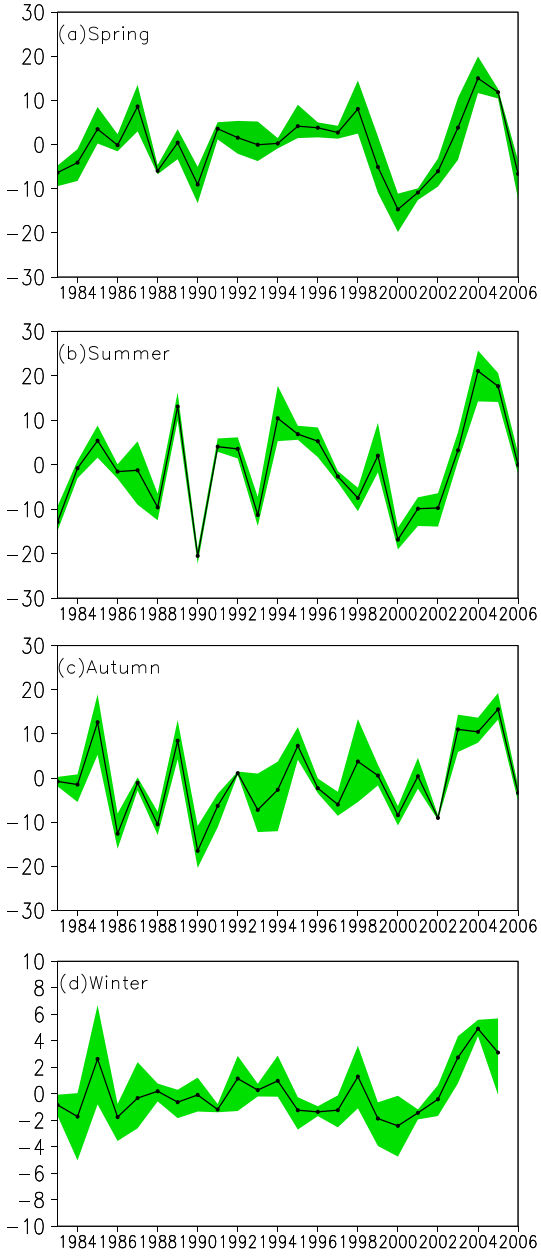

Figure 11. Annual variation of the mean seasonal *ET* anomaly (mm) (relative to the period of 1983–2006) from the corrected GLDAS2_ET, Zhang_ET, and JRA_ET for the upper Yellow River basin: (a) spring, (b) summer, (c) autumn, and (d) winter. The shades indicate the range determined by the three *ET* products. The linear trends of the mean *ET*, precipitation, runoff, and air temperature are given in Table 4.

ET for the two river basins (by equation (1)) and the two inland basins (by equation (2)). The reference *ET* shows a clear seasonal cycle with maxima in summer and minima in winter. The maxima for the upper Yellow River basin are generally larger than those for the upper Yangtze River basin. In the Qiangtang Plateau, the maxima are consistently larger than those for the Qaidam Basin. The variability of *ET* is dominant by the seasonal cycles of precipitation and runoff on the two river basins as well as precipitation on the two inland basins.

The monthly time series from the five *ET* products are also shown in Figure 4 and are compared with the reference *ET* for the four basins (Table 3). The five *ET* products exhibit substantial differences. For the upper Yellow River basin, all the *ET* products reproduce the seasonal cycles well, although the BIAS and RMSE are very different, with a range of −0.8–10.5 mm for BIAS and 5.5–17.1 mm for RMSE. Overall, GLDAS2_ET and Zhang_ET perform well with smaller BIAS/RMSE (−1.2/7.1 mm for GLDAS2_ET and −0.8/5.5 mm for Zhang_ET) and higher correlation coefficients (0.97 for GLDAS2_ET and 0.95 for Zhang_ET), while MODIS_ET is of relatively poor quality with the largest RMSE and the smallest correlation coefficient among the five ET products. GLDAS1_ET and JRA_ET's performance is moderate.

For the upper Yangtze River basin, Zhang_ET is the best at reproducing monthly variations, with relatively small BIAS and RMSE. Both GLDAS1_ET and GLDAS2_ET underestimate *ET*, but they reproduce the monthly variation fairly well with relatively high correlation coefficients (0.92 for GLDAS1_ET and 0.95 for GLDAS2_ET). Similar to the upper Yellow River basin, MODIS_ET and JRA_ET overestimate *ET* to a large extent. JRA_ET has a high correlation coefficient with the reference *ET*, demonstrating that the product reproduces monthly variations better than MODIS_ET. A previous study [*Xue et al.*, 2013] had discussed possible reasons for differences among several *ET* products for the upper Yellow and Yangtze River basins, which suggested that the underestimation of GLDAS2_ET was mainly caused by its negative bias for precipitation, whereas the overestimation of JRA_ET was due to the overestimation of downward shortwave radiation. Due to high downward shortwave radiation flux inputs from the Global Modeling and Assimilation Office, MODIS_ET greatly overestimated *ET* in both basins.

The comparisons of Zhang_ET and MODIS_ET with the reference *ET* cannot be done for the Qiangtang Plateau and Qaidam Basin because of the lack of estimates for the two basins. On the Qiangtang Plateau, GLDAS2_ET and JRA_ET fairly realistically reproduce the monthly variations of *ET* with correlation

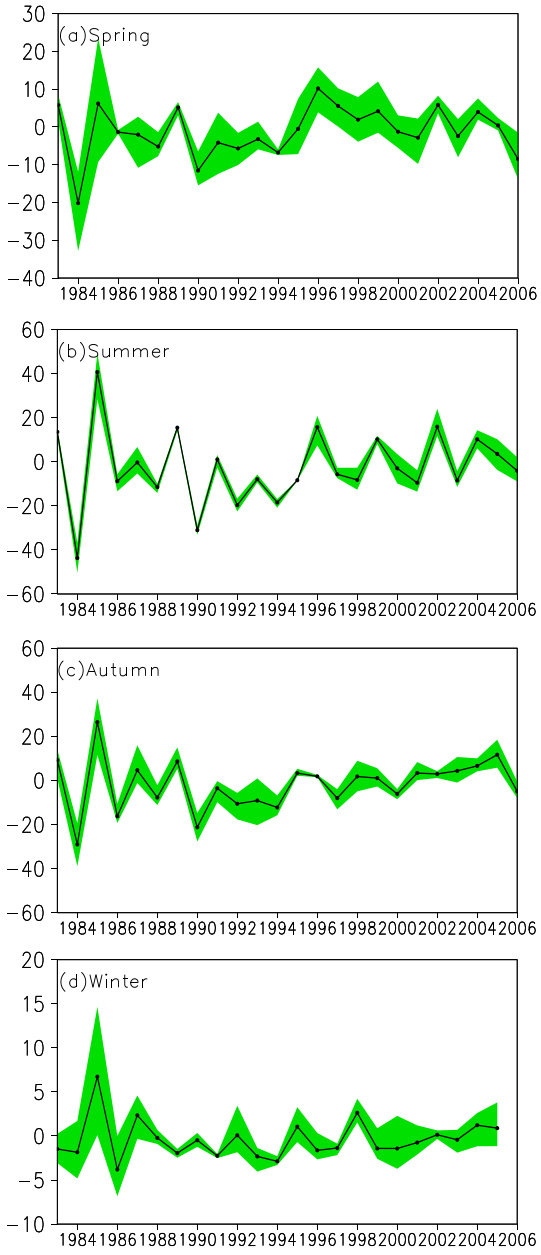

Figure 12. The same as Figure 11 but for the upper Yangtze River basin.

coefficients higher than 0.91, but there are larger BIAS and RMSE values for JRA_ET. By comparison, GLDAS1_ET displays relatively poor performance in reproducing the monthly *ET* variability. For the Qaidam Basin, GLDAS1_ET and GLDAS2_ET show similar performance, and JRA_ET follows them.

3.2. Probability Distribution Fitting

From the above analyses, all the *ET* products have poor performance in reproducing the maxima in summer and to some extent also the minima in winter. The gamma distribution has been proven to be effective presentation of precipitation [e.g., *Piani et al.*, 2010; *Liao et al.*, 2004] and evapotranspiration [e.g., *Bouraoui et al.*, 1999]. To examine the distribution of *ET* values from the five products, the gamma distribution [*Thom*, 1958], with shape parameter α and scale parameter β (by equation (6)), is assumed to be suitable for *ET* over the four basins with parameters determined on a monthly scale.

$$f_\gamma(x|\alpha,\beta) = x^{\alpha-1}\frac{1}{\beta^\alpha\Gamma(\alpha)}e^{\frac{-x}{\beta}}; x \geq 0; \alpha,\beta > 0 \qquad (6)$$

In this study, the cumulative distribution functions (CDFs) are constructed for the reference *ET* and the five *ET* products over the four basins for all months within the period of 2003–2012 (Figure 5). Except for MODIS_ET, all *ET* products display similar CDF compared with that of the reference *ET*. The differences between the five *ET* products and the reference *ET* are mainly caused by the biases in the *ET* estimates.

3.3. Bias Correction of *ET* Products

To improve the accuracy of *ET* products at the monthly scale, a bias correction is performed to all the *ET* products. The bias correction includes two steps. The first step is to use the gamma distribution of the reference *ET* during 2003 and 2012 to correct the distribution of the *ET* products. A schematic diagram to demonstrate the correction procedure is shown in Figure 6.

First, the gamma distribution (F_γ) is fitted to the monthly reference *ET* over the period of 2003–2012, which creates two parameters ($\alpha_{\text{reference}}$, $\beta_{\text{reference}}$). Then, the same gamma distribution is applied to the monthly *ET* values of each product during 2003 and 2012 to get the corresponding CDFs. With the mean distribution mapping of the reference *ET* ($\alpha_{\text{reference}}$, $\beta_{\text{reference}}$), the inverse function (F_γ^{-1}) is used to get the corrected values by means of the CDFs. This procedure can be expressed mathematically in terms of the gamma CDF (F_γ) and its inverse (F_γ^{-1}) as

$$ET_{\text{corrected}} = F_\gamma^{-1}\left(F_\gamma\left(ET_{\text{product}}|\alpha_{\text{product}},\beta_{\text{product}}\right)|\alpha_{\text{reference}},\beta_{\text{reference}}\right) \qquad (7)$$

The second step of the bias correction method is to eliminate annual bias using the ratio of annual reference *ET* to annual values from the *ET* products obtained in the first step using equation (8).

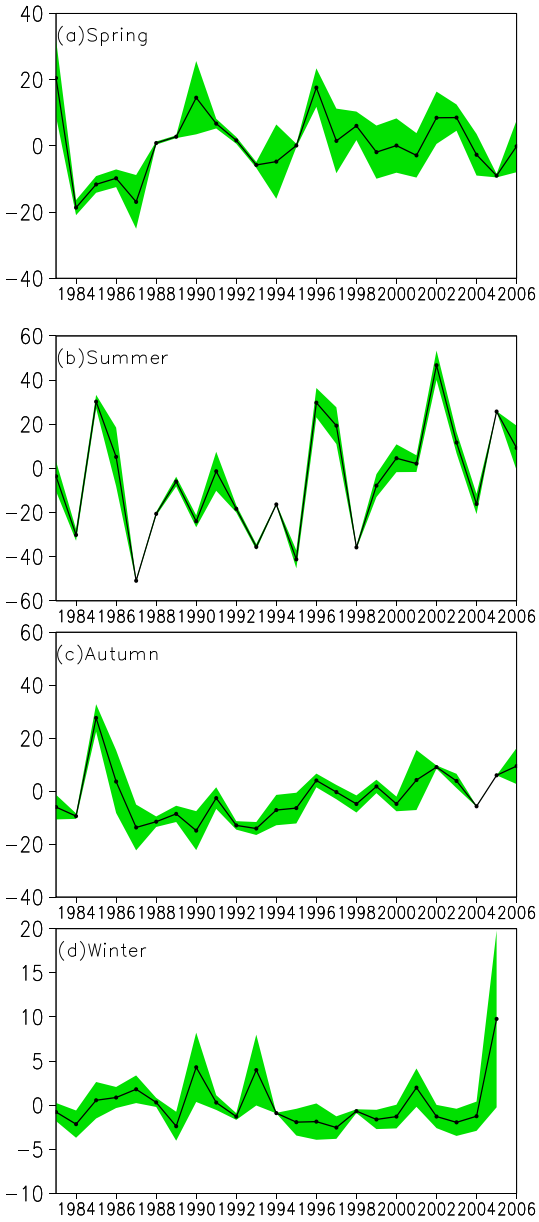

Figure 13. Annual variation of the mean seasonal *ET* anomaly (mm) (relative to the period of 1983–2006) from the corrected GLDAS2_ET and JRA_ET for the Qiangtang Plateau: (a) spring, (b) summer, (c) autumn, and (d) winter. The shades indicate the range determined by the two *ET* products. The linear trends of the mean *ET*, precipitation, and air temperature are given in Table 4.

$$ET_{\text{final}}(m) = \frac{(P_{\text{annual}} - R_{\text{annual}})}{ET_{\text{corrected}}(a)} \times ET_{\text{corrected}}(m) \quad (8)$$

where $ET_{\text{corrected}}(m)$ and $ET_{\text{corrected}}(a)$ represent the monthly and annual total *ET* from the *ET* products, respectively; P_{annual} and R_{annual} are the observed annual total *P* and *R* for the river basins; and the difference between P_{annual} and R_{annual} is the annual reference *ET*. For the Qiangtang Plateau and Qaidam Basin, R_{annual} is zero, and P_{annual} is equal to the annual reference *ET*. $ET_{\text{final}}(m)$ is the final corrected *ET* values for each *ET* product. The bias correction ensures that the corrected monthly *ET* products follow the gamma distribution of the reference *ET* and agree with interannual variation of the reference *ET*.

To evaluate the performance of the bias correction, comparisons between the reference *ET* and the five *ET* products before and after the bias correction for the four basins are carried out. The corresponding fittings and the statistical values are shown in Figure 7. After the bias correction, all the corrected *ET* products, except the GLDAS1_ET on the Qiangtang Plateau, show improved error statistics with reduced RMSE and higher correlation coefficients. Moreover, all the biases have been practically removed due to the correction, showing the effectiveness of the bias correction.

The comparisons of seasonal cycles among the *ET* products before and after the bias correction and the reference *ET* are shown in Figure 8. The root-mean-square error (RMSE) is used to evaluate the performance. It was obvious that the correction effectively removed the bias and reduced RMSE for all products except GLDAS1_ET for the Qiangtang Plateau. As a result, the seasonal cycles after the correction are much more realistic as compared with the reference.

In order to evaluate the ability of the *ET* products before and after the bias correction in capturing the interannual variability, Figure 9 shows the variation of correlation coefficient of seasonal mean reference *ET* with the five *ET* products over the four basins for the period of 2003–2012. It was found that the bias correction also helped in improving the ability of nearly all the *ET* products to capture the interannual variability of seasonal means. Thus, we will use the bias-corrected *ET* values to detect the long-term variability.

3.4. Water Balance Analysis

Among the five *ET* products, Zhang_ET, GLDAS2_ET, and JRA_ET use a continuous forcing data set as input for the periods of 1983–2006, 1948–2010, and 1979–2012, respectively. While MODIS_ET data are only available for a shorter period (2000–2012), GLDAS1_ET uses a constantly changing forcing data set as input, which is

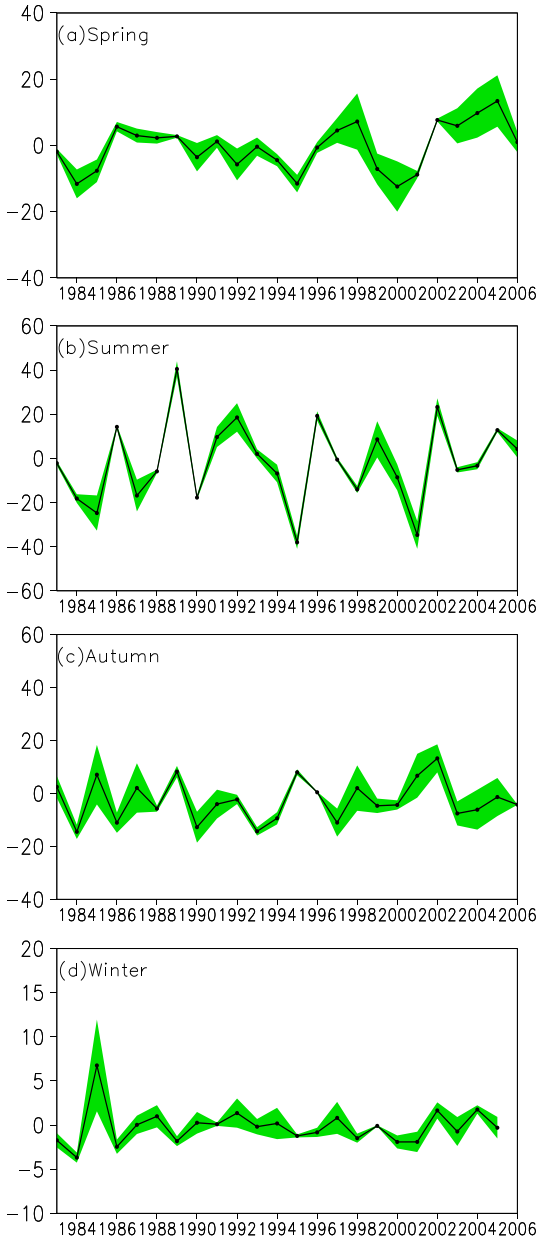

Figure 14. The same as Figure 13 but for the Qaidam Basin.

unsuited for detecting the long-term trend. Here three data sets (GLDAS2_ET, JRA_ET, and Zhang_ET) are selected to further detect seasonal trends of *ET* over the four basins for the common period (1983–2006). It should be noted that Zhang_ET does not have data for Qiangtang Plateau and Qaidam Basin, and only two data (GLDAS2_ET and JRA_ET) have full coverage.

To further demonstrate the consistency of the bias-corrected *ET* values, correlations among the three corrected *ET* products (Zhang_ET, GLDAS2_ET, and JRA_ET) in the same period of 1983–2006 are shown in Figure 10. The three corrected *ET* products indeed reproduce similar interannual variability, and the correlation coefficient between GLDAS2_ET and JRA_ET is the highest among all the correlation coefficients of the three products. The highest correlation coefficients are found in summer and autumn, followed by spring and then winter. This comparison implies that the corrected *ET* products provide more confidence for understanding the trends of *ET* and the impact of climate change on water balance, especially in warm seasons.

Water balance analyses for the four basins were carried out for the common period of 1983–2006 based on the observed *P*, *R*, and the mean *ET* data averaged over the corrected Zhang_ET, GLDAS2_ET, and JRA_ET data. Figures 11–14 show the range and mean of the three *ETs*, while Table 4 provides the estimated linear trends of the seasonal mean *P*, *R*, *ET*, and T_{air}.

For the upper Yellow River basin, the annual average *ET* and *R* make up 69% and 31% of the total available water (*P*), respectively. Although *P* in spring, autumn, and winter has an increasing trend, a strong decreasing trend in summer caused an annual decreasing *P* trend of −0.8 mm/decade. Four season mean *R* has a negative trend, which is more prominent in spring, summer, and winter than that in autumn. Changes in *R* for the basin are sensitive to *P*, with a correlation coefficient of 0.80 between annual *P* and R, which confirms the dominant role of *P* on *R* over this region [*Zhou and Huang*, 2012; *Zhang et al*., 2011]. For this region, *R* tended to decrease in summer and autumn as a result of evapotranspiration losses exceeding precipitation supply [*Liu et al*., 2012], while the decreasing of *R* in spring and winter is possibly dominated by the variation of ΔS. Additionally, the influence of human activities on the water budget over this region is negligible. However, the degenerating frozen soil, which caused more water infiltration, may be another reason for the decrease in *R* for this region [*Zhou and Huang*, 2006].

For the upper Yangtze River basin, the annual average *ET* and *R* make up 75% and 25% of the total *P*, respectively, which is different from the upper Yellow River basin due to different geographic settings. Except for *R* in spring-summer, seasonal mean *P*, *R*, and *ET* all have increased, but only the changes in *P* in

Table 4. Linear Trends of Annual and Seasonal Mean Precipitation (P: mm decade^{-1}), Runoff (R: mm decade^{-1}), Bias-Corrected Evapotranspiration (ET: mm decade^{-1}) and Air Temperature (T_{air}: °C decade^{-1}) for the Four Basins Under the Period of 1983–2006[a]

	Yellow				Yangtze				Qiangtang				Qaidam			
	Spring	Summer	Autumn	Winter	Spring	Summer	Autumn	Winter	Spring	Summer	Autumn	Winter	Spring	Summer	Autumn	Winter
P	1.7	−9.0	2.4	4.2	8.0	12.8	3.0	2.3	11.1	15.0	2.7	3.3	4.1	13.9	6.0	2.0
R	−4.3	−17.4	−6.5	−1.4	−0.5	−0.9	2.9	0.0	/	/	/	/	/	/	/	/
ET	0.7	3.4	3.4	0.7	0.2	2.4	3.4	0.0	2.3	11.9	3.9	0.5	3.1	2.4	1.1	0.2
T_{air}	0.4	0.6	0.5	0.7	0.4	0.7	0.7	1.0	0.5	0.5	0.6	0.9	0.7	0.9	0.7	0.8

[a]Underlined trends indicate that they are statistically significant at the 95% significant level.

spring and winter are significant at the 95% significant level. The annual mean P correlates well with the annual mean R and the annual mean ET, with correlation coefficients of 0.76 and 0.91, respectively, which means that the changes in P to a large extent determine the changes in R and ET. Moreover, some previous study found that glacier melting due to warming is another reason for the increasing R over this region during the 21st century [e.g., *Bai and Rong*, 2012].

Recent studies about increasing temperature trends at higher elevations on the Qinghai-Tibetan Plateau [*Liu and Chen*, 2000; *Qin et al*., 2009; *Wang et al*., 2011] also happen on the Qiangtang Plateau, with a value of 0.9°C decade^{-1} in winter season. The maxima trends of P and ET appear in summer for the Qiangtang Plateau during the period of 1983–2006. For the Qaidam Basin, there are maxima trends of P in summer, while the maxima trends of ET appear in spring. Located in the semiarid and subhumid region, the Qaidam Basin has 60% of the annual precipitation in the summer. Therefore, the concentrated summer precipitation may have produced the infiltration access runoff, which leads to less contribution to ET. This means that the maxima trends of P in summer do not necessarily lead to maxima of ET in summer in this basin.

4. Summary and Conclusions

Evapotranspiration data from five global sources were evaluated for four large basins of the Tibetan Plateau against the ET estimated by the water balance method (reference ET) at monthly scale. During the comparison period (2003–2012), the five ET products display varying, sometimes substantial, differences compared with the reference ET, despite similar seasonal variations.

A bias correction method, based on the probability distribution mapping, was applied to the five ET products at monthly scales. Compared with the reference ET, the correction not only effectively removed the biases but also substantially reduced RMSEs and improved temporal variations, especially the seasonal cycle. Therefore, the corrected ET products are considered reasonable and of high quality, which adds confidence for the further trend analysis.

Surface water balance changes in the four basins for the period of 1983–2006 are then analyzed using the corrected ET from GLDAS2_ET, JRA_ET, and Zhang_ET as well as observed P and R. In the upper Yellow River basin, there is a general increasing trend for ET in all seasons, especially for summer and autumn, along with the warming trend in the basin. For the upper Yangtze River basin, P and ET also show increasing trends in all the seasons, while R decreased in spring and summer and increased in autumn and winter. Moreover, P and ET for the Qiangtang Plateau and Qaidam Basin increased in all seasons. It is interesting to note that while there are dominating positive trends for P, dominating negative trends for R, and all positive trends for T_{air} on the seasonal basis for all the four basins, ET shows a positive seasonal trend for all the seasons and basins.

Acknowledgments
This study was supported financially by the National Key Basic Research Program of China (2013CBA018), the "Strategic Priority Research Program" of the Chinese Academy of Sciences (XDB03030302), the National Natural Science Foundation of China (grants 41322001, 41190083, and 41405076), and the Hundred Talents Program of Chinese Academy of Sciences (Lei Wang). We are also grateful for the GRACE land data (available at http://grace.jpl.nasa.gov) processing algorithms that were provided by Sean Swenson and supported by the NASA MEaSUREs Program. Deliang Chen is also supported by the Swedish program Modelling the Regional and Global Earth system, and Biodiversity and Ecosystem services in a Changing Climate.

References

Bai, L. Y., and Y. S. Rong (2012), Impacts of climate change on water resources in source regions of Yangtze River and Yellow River [in Chinese with English abstract], *Water Resour. Protect.*, *28*(1), 46–70.

Bing, L. F., Q. Q. Shao, and J. Y. Liu (2012), Runoff characteristics in flood and dry seasons based on wavelet analysis in the source regions of the Yangtze and Yellow rivers, *J. Geogr. Sci.*, *22*(2), 261–272.

Bouraoui, F., G. Vachaud, L. Z. X. Li, H. LeTreut, and T. Chen (1999), Evaluation of the impact of climate changes on water storage and groundwater recharge at the watershed scale, *Clim. Dyn.*, *15*(2), 153–161.

Brutsaert, W., and M. B. Parlange (1998), Hydrologic cycle explains the evaporation paradox, *Nature*, *396*(6706), 30, doi:10.1038/23845.
Chen, D., G. Gao, C. Y. Xu, J. Guo, and G. Y. Ren (2005), Comparison of the Thornthwaite method and pan data with the standard Penman-Monteith estimates of reference evapotranspiration in China, *Clim. Res.*, *28*(2), 123–132.
Ferguson, C. R., J. Sheffield, E. F. Wood, and H. Gao (2010), Quantifying uncertainty in a remote sensing-based estimate of evapotranspiration over continental USA, *Int. J. Remote Sens.*, *31*(14), 3821–3865.
Gao, G., D. Chen, C. Y. Xu, and E. Simelton (2007), Trend of estimated actual evapotranspiration over China during 1960-2002, *J. Geophys. Res.*, *112*, D11120, doi:10.1029/2006JD008010.
Gao, H. L., Q. H. Tang, C. R. Ferguson, E. F. Wood, and D. P. Lettenmaier (2010), Estimating the water budget of major US river basins via remote sensing, *Int. J. Remote Sens.*, *31*(14), 3955–3978.
Golubev, V. S., J. H. Lawrimore, P. Y. Groisman, N. A. Speranskaya, S. A. Zhuravin, M. J. Menne, T. C. Peterson, and R. W. Malone (2001), Evaporation changes over the contiguous United States and the former USSR: A reassessment, *Geophys. Res. Lett.*, *28*(13), 2665–2668, doi:10.1029/2000GL012851.
He, J., and K. Yang (2011), China Meteorological Forcing Dataset, Cold and Arid Regions Science Data Center at Lanzhou, doi:10.3972/westdc.002.2014.db.
Hobbins, M. T., J. A. Ramírez, and T. C. Brown (2004), Trends in pan evaporation and actual evapotranspiration across the conterminous U.S.: Paradoxical or complementary?, *Geophys. Res. Lett.*, *31*, L13503, doi:10.1029/2004GL019846.
Huntington, T. G. (2006), Evidence for intensification of the global water cycle: Review and synthesis, *J. Hydrol.*, *319*(1–4), 83–95.
Immerzeel, W. W., L. P. H. van Beek, and M. F. P. Bierkens (2010), Climate Change Will Affect the Asian Water Towers, *Science*, *328*(5984), 1382–1385.
Intergovernmental Panel on Climate Change Fifth Assessment Report (IPCC AR5) (2013), Summary for Policymakes: The Physical Science Basis, Contribution of Working Group I to the IPCC Fifth Assessment Report Climate Change. [Available at http://www.climatechange2013.Org/images/upload/WGIAR5-SPM_Approved27Sep2013.pdf.]
Klees, R., E. A. Zapreeva, H. C. Winsemius, and H. H. G. Savenije (2007), The bias in GRACE estimates of continental water storage, *Hydrol. Earth Syst. Sci.*, *11*, 1227–1241, doi:10.5194/hess-11-1227-2007.
Landerer, F. W., and S. C. Swenson (2012), Accuracy of scaled GRACE terrestrial water storage estimates, *Water Resour. Res.*, *48*, W04531, doi:10.1029/2011WR011453.
Lawrimore, J. H., and T. C. Peterson (2000), Pan evaporation trends in dry and humid regions of the United States, *J. Hydrometeorol.*, *1*(6), 543–546.
Liao, Y. M., Q. Zhang, and D. Chen (2004), Stochastic modeling of daily precipitation in China, *J. Geogr. Sci.*, *14*(4), 417–426.
Liu, C. H., W. J. Su, and Y. H. Yang (2012), Impacts of Climate change on the runoff and estimation on the future climatic trends in the headwater regions of the Yellow River, *J. Arid Land Res. Environ.*, *26*(4), 97–101.
Liu, X. D., and B. D. Chen (2000), Climatic warming in the Tibetan Plateau during recent decades, *Int. J. Climatol.*, *20*(14), 1729–1742.
Liu, X. M., H. X. Zheng, M. H. Zhang, and C. M. Liu (2011), Identification of dominant climate factor for pan evaporation trend in the Tibetan Plateau, *J. Geogr. Sci.*, *21*(4), 594–608.
Long, D., L. Longuevergne, and B. R. Scanlon (2014), Uncertainty in evapotranspiration from land surface modeling, remote sensing, and GRACE satellites, *Water Resour. Res.*, *50*, 1131–1151, doi:10.1002/2013WR014581.
Longuevergne, L., B. R. Scanlon, and C. R. Wilson (2010), GRACE hydrological estimates for small basins: Evaluating processing approaches on the High Plains aquifer, USA, *Water Resour. Res.*, *46*, W11517, doi:10.1029/2009WR008564.
Mu, Q., F. A. Heinsch, M. Zhao, and S. W. Running (2007), Development of a global evapotranspiration algorithm based on MODIS and global meteorology data, *Remote Sens. Environ.*, *111*(4), 519–536.
Nakaegwa, T. (2008), Reproducibility of the seasonal cycles of land-surface hydrological variables in Japanese 25-year Reanalysis, *Hydrol. Res. Lett.*, *8*(2), 56–60.
Ohmura, A., and M. Wild (2002), Is the hydrological cycle accelerating?, *Science*, *298*(5597), 1345–1356, doi:10.1126/science.1078972.
Onogi, K., et al. (2007), The JRA-25 Reanalysis, *J. Meteorol. Soc. Jpn., Ser. II*, *85*(3), 369–432.
Piani, C., J. O. Haerter, and E. Coppola (2010), Statistical bias correlation for daily precipitation in regional climate models over Europe, *Theor. Appl. Climatol.*, *99*(1–2), 187–192.
Qin, J., K. Yang, S. Liang, and X. Guo (2009), The altitudinal dependence of recent rapid warming over the Tibetan Plateau, *Clim. Change*, *97*(1–2), 321–327.
Ramillien, G., F. Frappart, A. Guntner, T. Ngo-Duc, A. Cazenave, and K. Laval (2006), Time variations of the regional evapotranspiration rate from Gravity Recovery and Climate Experiments (GRACE) satellit gravimetry, *Water Resour. Res.*, *42*, W10403, doi:10.1029/2005WR004331.
Rana, G., and N. Katerji (2000), Measurement and estimation of actual evapotranspiration in the field under Mediterranean climate: A review, *Eur. J. Agron.*, *13*(2–3), 125–153, doi:10.1016/S1161-0301(00)00070-8.
Rodell, M., and J. S. Famiglietti (1999), Detectability of variations in continental water storage from satellite observations of the time dependent gravity field, *Water Resour. Res.*, *35*(9), 2705–2723, doi:10.1029/1999WR900141.
Rodell, M., and J. S. Famiglietti (2002), The potential for satellite-based monitoring of groundwater storage changes using GRACE: The High Plains aquifer, Central US, *J. Hydrol.*, *263*(1–4), 245–256.
Rodell, M., et al. (2004a), The Global Land Data Assimilation System, *Bull. Am. Meteorol. Soc.*, *85*(3), 381–394.
Rodell, M., J. S. Famiglietti, J. Chen, S. I. Seneviratne, P. Viterbo, S. Holl, and C. R. Wilson (2004b), Basin scale estimates of evapotranspiration using GRACE and other observations, *Geophys. Res. Lett.*, *31*, L20504, doi:10.1029/2004GL020873.
Sheffield, J., G. Goteti, and E. F. Wood (2006), Development of a 50-yr high-resolution global dataset of meteorological forcings for land surface modeling, *J. Clim.*, *19*(13), 3088–3111.
Sheffield, J., C. R. Ferguson, T. J. Troy, E. F. Wood, and M. F. McCabe (2009), Closing the terrestrial water budget from satellite remote sensing, *Geophy. Res. Lett.*, *36*, L07403, doi:10.1029/2009GL037338.
Su, F., X. Duan, D. Chen, Z. Hao, and C. Lan (2013), Evaluation of the global climate models in the cmip5 over the Tibetan Plateau, *J. Clim.*, *26*, 3187–3208.
Swenson, S., and J. Wahr (2002), Methods for inferring regional surface-mass anomalies from GRACE measurements of time- variable gravity, *J. Geophys. Res.*, *107*(B9), 2193, doi:10.1029/2001JB000576.
Swenson, S. C., and J. Wahr (2006a), Estimating Large-Scale Precipitation Minus Evapotranspiration from GRACE Satellite Gravity Measurements, *J. Hydrometeorol.*, *7*(2), 252–270, doi:10.1175/JHM478.1.
Swenson, S. C., and J. Wahr (2006b), Post-processing removal of correlated errors in GRACE data, *Geophys. Res. Lett.*, *33*, L08402, doi:10.1029/2005GL025285.
Swenson, S., P. J.-F. Yeh, J. Wahr, and J. Famiglietti (2006), A comparison of terrestrial water storage variations from GRACE with in situ measurements from Illinois, *Geophys. Res. Lett.*, *33*, L16401, doi:10.1029/2006GL026962.

Takahashi, K., N. Yamazaki, and H. Kamahori (2006), Trends of heavy precipitation events in global observation and reanalysis datasets, *Sci. Online Lett. Atmos.*, *2*, 96–99.

Tang, Q. H., X. J. Zhang, and Y. Tang (2013), Anthropogenic impacts on mass change in North China, *Geophys. Res. Lett.*, *40*, 3924–3928, doi:10.1002/grl.50790.

Tapley, B. D., S. Bettadpur, J. C. Ries, P. F. Thompson, and M. M. Watkins (2004), GRACE Measurements of Mass Variability in the Earth System, *Science*, *305*(5683), 503–505.

Thom, H. C. S. (1958), A note on the gamma distribution, *Mon. Weather Rev.*, *86*(4), 117–122.

Tosiyuki, N. (2008), Reproducibility of the season cycles of land-surface hydrological variables in Japanese 25-year Reanalysis, *Hydrol. Res. Lett.*, *2*, 56–60.

Vinukollu, R. K., R. Meynadier, J. Sheffield, and E. F. Wood (2011a), Multi-model, multi-sensor estimates of global evapotranspiration: Climatology, uncertainties and trends, *Hydrol. Processes*, *25*(26), 3993–4010.

Vinukollu, R. K., E. F. Wood, C. R. Ferguson, and J. B. Fisher (2011b), Global estimates of evapotranspiration for climate studies using multi-sensor remote sensing data: Evaluation of three process-based approaches, *Remote Sens. Environ.*, *115*(3), 801–823.

Wahr, J., S. Swenson, I. Velicogna, and V. Zlotnicki (2004), Time-variable gravity from GRACE: First results, *Geophys. Res. Lett.*, *31*, L11501, doi:10.1029/2004GL019779.

Wang, K. C., and R. E. Dickinson (2012), A review of global terrestrial evapotranspiration: Observation, modeling, climatology, and climatic variability, *Rev. Geophys.*, *50*, RG2005, doi:10.1029/2011RG000373.

Wang, K. L., J. Song, G. D. Cheng, and H. Jiang (2011), Effect of altitude and latitude on surface air temperature across the Qinghai-Tibet Plateau, *J. Mt. Sci.*, *8*(6), 808–816.

Xu, C. Y., and V. P. Singh (2005), Evaluation of three complementary relationship evapotranspiration model by water balance approach to estimate actual regional evapotranspiration in different climatic regions, *J. Hydrol.*, *308*(1–4), 105–121, doi:10.1016/j.jhydrol.2004.10.024.

Xu, C. Y., L. B. Gong, T. Jiang, and D. Chen (2006), Decreasing reference evapotranspiration in a warming climate-A case of Changjiang (Yangtze) River Catchment during 1970-2000, *Adv. Atmos. Sci.*, *23*(4), 513–520.

Xue, B. L., L. Wang, X. P. Li, K. Yang, D. L. Chen, and L. T. Sun (2013), Evaluation of evapotranspiration estimates for two river basins on the Tibetan Plateau by a water balance method, *J. Hydrol.*, *492*(7), 290–297.

Yang, K., B. S. Ye, D. G. Zhou, B. Y. Wu, T. Foken, J. Qin, and Z. Y. Zhou (2011), Response of hydrological cycle to recent climate changes in the Tibetan Plateau, *Clim. Change*, *109*(3–4), 517–534, doi:10.1007/s10584-011-0099-4.

Yao, T. D., et al. (2012), Different glacier status with atmospheric circulations in Tibetan Plateau and surroundings, *Nat. Clim. Change*, *2*(9), 663–667.

Yeh, P. J. F., S. C. Swenson, J. S. Famiglietti, and M. Rodell (2006), Remote sensing of groundwater storage changes in Illinois using the Gravity Recovery and Climate Experiment (GRACE), *Water Resour. Res.*, *42*, W12203, doi:10.1029/2006WR005374.

Zhang, K., J. S. Kimball, R. R. Nemani, and S. W. Running (2010), A continuous satellite-derived global record of land surface evapotranspiration from 1983 to 2006, *Water Resour. Res.*, *46*, W09522, doi:10.1029/2009WR008800.

Zhang, S. F., D. Hua, X. J. Meng, and Y. Y. Zhang (2011), Climate change and its driving effect on the runoff in the "Three-River Headwaters" region, *J. Geogr. Sci.*, *21*(6), 963–978, doi:10.1007/s11442-011-0893-y.

Zhang, Y. Q., C. M. Liu, Y. H. Tang, and Y. H. Yang (2007), Trends in pan evaporation and reference and actual evapotranspiration across the Tibetan Plateau, *J. Geophys. Res.*, *112*, D12110, doi:10.1029/2006JD008161.

Zhou, D. G., and R. H. Huang (2006), Exploring of reason of runoff decrease in the source regions of the Yellow River [in Chinese with English abstract], *Clim. Environ. Res.*, *11*(3), 302–309.

Zhou, D. G., and R. H. Huang (2012), Response of water budget to recent climatic changes in the source region of the Yellow River, *Chin. Sci. Bull.*, *57*(17), 2155–2162.